

<https://doi.org/10.1038/s42003-024-06202-9>

Wnt/ β -catenin signaling regulates amino acid metabolism through the suppression of CEBPA and FOXA1 in liver cancer cells

Check for updates

Saya Nakagawa¹, Kiyoshi Yamaguchi¹ ✉, Kiyoko Takane¹, Sho Tabata², Tsuneo Ikenoue¹ & Yoichi Furukawa¹ ✉

Deregulation of the Wnt/ β -catenin pathway is associated with the development of human cancer including colorectal and liver cancer. Although we previously showed that histidine ammonia lyase (*HAL*) was transcriptionally reduced by the β -catenin/TCF complex in liver cancer cells, the mechanism(s) of its down-regulation by the complex remain to be clarified. In this study, we search for the transcription factor(s) regulating *HAL*, and identify CEBPA and FOXA1, two factors whose expression is suppressed by the knockdown of β -catenin or TCF7L2. In addition, RNA-seq analysis coupled with genome-wide mapping of CEBPA- and FOXA1-binding regions reveals that these two factors also increase the expression of arginase 1 (*ARG1*) that catalyzes the hydrolysis of arginine. Metabolome analysis discloses that activated Wnt signaling augments intracellular concentrations of histidine and arginine, and that the signal also increases the level of lactic acid suggesting the induction of the Warburg effect in liver cancer cells. Further analysis reveals that the levels of metabolites of the urea cycle and genes coding its related enzymes are also modulated by the Wnt signaling. These findings shed light on the altered cellular metabolism in the liver by the Wnt/ β -catenin pathway through the suppression of liver-enriched transcription factors including CEBPA and FOXA1.

Alterations in the genes associated with the Wnt/ β -catenin signaling pathway have been identified in various types of tumors¹. In colorectal cancer, over 90% of the cases carry at least one mutation in genes involved in this pathway such as inactivating mutations of the adenomatous polyposis coli (*APC*) gene (~80%) and activating mutations of the β -catenin (*CTNNB1*) gene (~5%)². In hepatocellular carcinoma (HCC), somatic mutations in *CTNNB1* (31%) and *AXIN1* (6%) have been frequently found³. These mutations result in the accumulation of β -catenin and its translocation into the nucleus to form transcriptionally active complexes with T-cell factor/lymphoid enhancer factor (TCF/LEF) family proteins. Importantly, genes directly transactivated by the complexes have been shown to play a key role in the development of tumors. For example, c-Myc and cyclin D1 regulate cell proliferation and/or cell cycle progression^{4,5}. Although more than one hundred target genes have been identified, most of the genes are transcriptionally up-regulated by the complex, and little attention have been paid to the down-regulated genes.

We previously reported that the suppressed expression of IRF1 by the signal plays a vital role in colorectal carcinogenesis, and its expression was regulated by the ubiquitin-proteasome pathway through a deubiquitinase complex, USP1/UAF1⁶. We also revealed that histidine ammonia-lyase (*HAL*), phosphoenolpyruvate carboxykinase 1 (*PCK1*), solute carrier family 51 subunit alpha (*SLC51A*), pleckstrin 2 (*PLEK2*), integrin β 3 (*ITGB3*), and secretory leukocyte protease inhibitor (*SLPI*) were transcriptionally down-regulated by the Wnt signaling pathway in liver cancer⁷. Additionally, we identified a regulatory region of *HAL*, between -90 bp and -44 bp in the 5'-flanking region, and revealed that transcriptional activity of the region was suppressed by the activation of Wnt/ β -catenin signaling⁷.

HAL is the rate-limiting enzyme of histidine catabolism and catalyzes L-histidine to urocanate and ammonia in the liver and skin. Histidine metabolism is an important metabolic process involved in de novo synthesis of purine nucleic acids that accelerates the cancer cell progression due to the association with production of tetrahydrofolate⁸. In addition, histamine, a metabolite converted from histidine, plays an important role in cancer

¹Division of Clinical Genome Research, Advanced Clinical Research Center, The Institute of Medical Science, The University of Tokyo, Tokyo 108-8639, Japan. ²Tsuruoka Metabolomics Laboratory, National Cancer Center, Tsuruoka, Yamagata 997-0052, Japan. ✉e-mail: kiyamagu@g.ecc.u-tokyo.ac.jp; yofurukawa@g.ecc.u-tokyo.ac.jp

immunity through the control of various responses in innate and adaptive immunity⁹. Although the expression of *HAL* may play a crucial role in cancer cells, the regulatory mechanism remains to be clarified.

Regarding the link between the canonical Wnt signaling and metabolism, it was reported that the activation of the Wnt signaling pathway induced the Warburg effect through increased expression of *MYC*¹⁰, *PDK1*¹¹, and lactate/pyruvate transporter *MCT1/SLC11A1*¹² or suppression of cytochrome oxidase¹³. Importantly, crosstalk between the Wnt and c-Myc pathways promotes glycolysis and energy production in cancer cells¹⁴. In addition, glycolysis modulates Wnt signaling to promote axial elongation of the embryo in the tail bud¹⁵, suggesting a tight link between Wnt signaling and aerobic glycolysis. However, little is known about the effect of Wnt signaling on other metabolisms.

In this study, we clarified that *HAL* was transcriptionally induced by *CEBPA* and *FOXA1*, and that their expression levels were down-regulated by the Wnt/ β -catenin signaling in the liver cancer cells. Furthermore, we found that activated Wnt/ β -catenin signaling suppressed not only *HAL* but also *ARG1*, a gene encoding arginase 1, through the reduced *CEBPA* and *FOXA1* expression. These data helped us gain insight into a role of the signal pathway in amino acid metabolism in liver cancer.

Results

Identification of candidate transcription factor(s) regulating *HAL* in liver cancer cells

We previously uncovered that the 5'-flanking region of *HAL*, between -90 bp and -44 bp, was responsible for the suppression of β -catenin/TCF complex in liver cancer cells⁷. Since the β -catenin/TCF complex induces downstream target genes, the decreased transcription of *HAL* was assumed to be indirectly regulated by the complex. In agreement with this notion, the region has no β -catenin/TCF7L2 ChIP-seq peaks or consensus TCF-binding motifs (ENCODE accession number: ENCSR000EVQ).

We searched for transcription factors (TFs) that are associated with the activity of the *HAL* 5'-flanking region using JASPAR, a database of TF-binding profiles (<http://jaspar.genereg.net/>). As a result, a total of 41 putative motifs including 33 TFs with a score of 8.0 or above were identified in the region (Supplementary Data 1a). We searched for two types of TFs among the 33 identified, namely transcriptional repressors that were up-regulated by the Wnt/ β -catenin pathway and activators that were down-regulated by the pathway. Expression profile analysis was performed using HepG2 hepatoblastoma cells transfected with different siRNAs targeting β -catenin (-9 or -10), TCF7, TCF7L1, TCF7L2, LEF1, or their combination (Supplementary Data 1b, c) and the expression levels of the 33 TFs were compared with those of downstream genes in the Wnt signaling pathway using the expression profile data (Supplementary Fig. 1a). As expected, *MYC*, *RNF43*, *AXIN2*, and *LGR5*, four well-known Wnt target genes were down-regulated by the treatment with β -catenin, TCF7L2, or TCF7 siRNA (Fig. 1a). However, TCF7L1 and LEF1 are unlikely to be involved in the activation of Wnt signaling in the cells, possibly due to the lower expression of TCF7L1 and LEF1 compared with other TCF family members in HepG2 cells. We additionally confirmed that *HAL* expression was remarkably enhanced by the treatment with β -catenin, TCF7L2, or TCF7 siRNA.

A hierarchical clustering analysis using expression values of the 33 TFs, *HAL*, and the four Wnt target genes identified subsets of genes that exhibited different expression patterns in response to the suppression of Wnt signaling (Fig. 1a). Intriguingly, *FOXD1* and *FOXP1* were classified in a subgroup containing the four Wnt target genes (*MYC*, *RNF43*, *AXIN2*, and *LGR5*), suggesting that these two genes may be up-regulated by the activation of Wnt signaling. *FOXD1* is known to be a transcriptional activator¹⁶, but *FOXP1* was reported to act primarily as a transcriptional repressor^{17,18}. Therefore, we included *FOXP1* as a candidate suppressor of *HAL*. Additional qPCR analysis confirmed that *FOXP1* expression was significantly decreased by the depletion of β -catenin- or TCF7L2 in HepG2 cells (Supplementary Fig. 1b). Although we treated HuH-7 cells with two-independent *FOXP1* siRNA, *HAL* expression was not induced by the

treatment (Supplementary Fig. 1c), suggesting that *FOXP1* may not suppress the transcription of *HAL* in the cells.

We additionally identified nine TFs including *CEBPA*, *FOXA1*, *FOXA3*, *FOXK1*, *FOXN3*, *FOXP3*, *NFATC2*, *PROX1*, and *SRY*, which were classified in a subgroup containing *HAL* by the cluster analysis, suggesting that these TFs are candidate transcriptional activator(s) regulating *HAL*. Among the nine TFs, we focused on factors whose expression was correlated with *HAL* in liver cancer tissues using the TCGA data (cBioportal, <https://www.cbioportal.org/>), because the negative regulation of *HAL* by Wnt signaling was most explicit in liver cancer, but not in colorectal cancer⁷. As a result, the expression levels of *FOXA3* ($r=0.36$), *FOXA1* ($r=0.25$), and *CEBPA* ($r=0.22$) were significantly correlated with those of *HAL* (q -value < 0.01 , Supplementary Fig. 2a). To validate the association of their expression with the Wnt signaling, we carried out qPCR and western blot analyses using HepG2 and HuH-6 cells carrying activating mutations in the *CTNNB1* (β -catenin) gene. As expected, silencing of β -catenin or TCF7L2 increased the expression of *CEBPA*, *FOXA1*, and *FOXA3* at the RNA and protein levels (Fig. 1b, c and Supplementary Fig. 2b). It is of note that these three TFs are known as liver-enriched TFs¹⁹, and that *HAL* and the three TFs are also abundantly expressed in normal liver tissue (Supplementary Fig. 2c, d). These data suggested that *CEBPA*, *FOXA1*, and *FOXA3* were candidates that transcriptionally regulate *HAL* expression (Supplementary Fig. 2e).

To investigate whether expression of the three factors was regulated in an Wnt/ β -catenin-dependent manner in liver cancer, we treated HuH-7 cells with a GSK-3 α / β inhibitor, CHIR-99021, and examined their expression. As a result, the treatment significantly down-regulated the expression of *CEBPA*, *FOXA1*, and *FOXA3* (Fig. 1d). In complete agreement with these results, TCGA data showed that HCCs carrying mutant *CTNNB1* have decreased expression of the three TFs as well as *HAL* compared to those with the wild-type (Fig. 1e). Taken together, these data strengthened our findings that *CEBPA*, *FOXA1*, and *FOXA3* are down-regulated by the Wnt signaling.

The effect of *CEBPA*, *FOXA1*, and *FOXA3* on the reporter activity of *HAL*

Next, we examined the interaction of the three TFs with the regulatory region between -90 bp and -44 bp of *HAL*. The JASPAR database suggested two CEBP-binding elements (CBE-1 and CBE-2) and a Forkhead-binding element (FBE) within the region to interact with both *FOXA1* and *FOXA3* (Supplementary Fig. 3a, b). To analyze whether these three elements are functionally associated with the transcriptional activity, we used a reporter plasmid containing the *HAL* promoter and its minimal regulatory region upstream of the firefly luciferase gene (pHAL-90/+147)⁷. We generated four mutant reporter plasmids (Fig. 2a), namely a three-base substitution in CBE-1 (CBE-1m), a two-base substitution in CBE-2 (CBE-2m), a three-base substitution in FBE (FBE m), and a combination of the three mutations (CBE-1m, CBE-2m, and FBE m). Reporter assay using the wild-type plasmids in combination with β -catenin siRNA confirmed that knockdown of β -catenin increased the wild-type reporter activity in HepG2 cells (Fig. 2b). The increase in wild type reporter activity by the β -catenin siRNA was partially reduced by the mutations of three binding motifs (CBE-1m, CBE-2m, and FBE m). Notably, the combination of the mutations in the three motifs almost abolished the increased reporter activity by the β -catenin siRNA. We additionally analyzed the reporter activity of the wild-type plasmids by over-expression of the three TFs in HepG2 cells. As a result, over-expression of *CEBPA* alone significantly augmented the reporter activity (Fig. 2c and Supplementary Fig. 4a). Furthermore, knockdown of *CEBPA* or *FOXA1* with two-independent siRNAs for each gene significantly decreased the reporter activity, but the activity was not changed by the knockdown of *FOXA3* (Fig. 2d).

CEBPA and *FOXA1* are bona fide regulators of the expression of *HAL*

To further investigate the involvement of these three TFs, we treated HuH-7 and Hep3B cells with *CEBPA*, *FOXA1*, or *FOXA3* siRNAs and

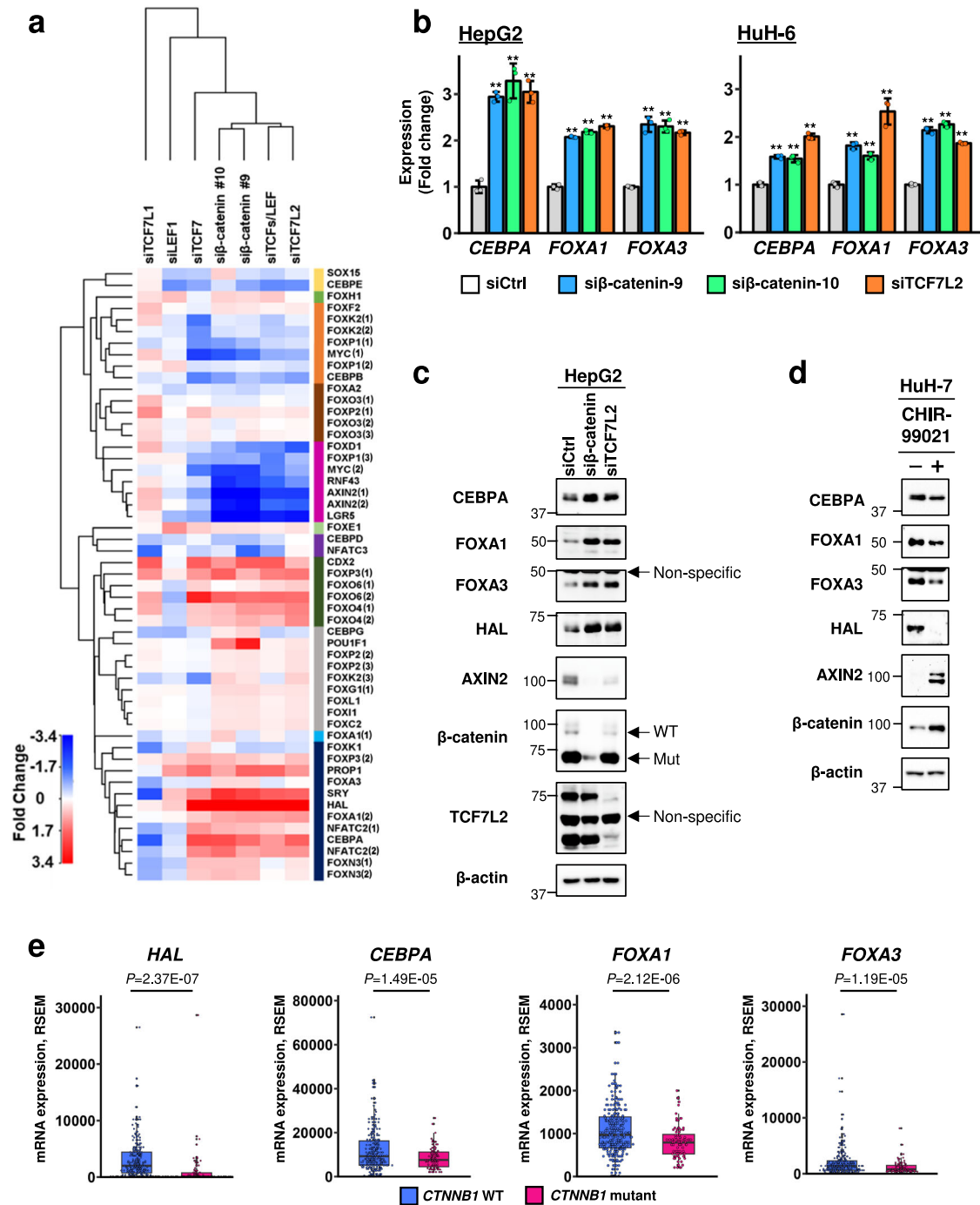
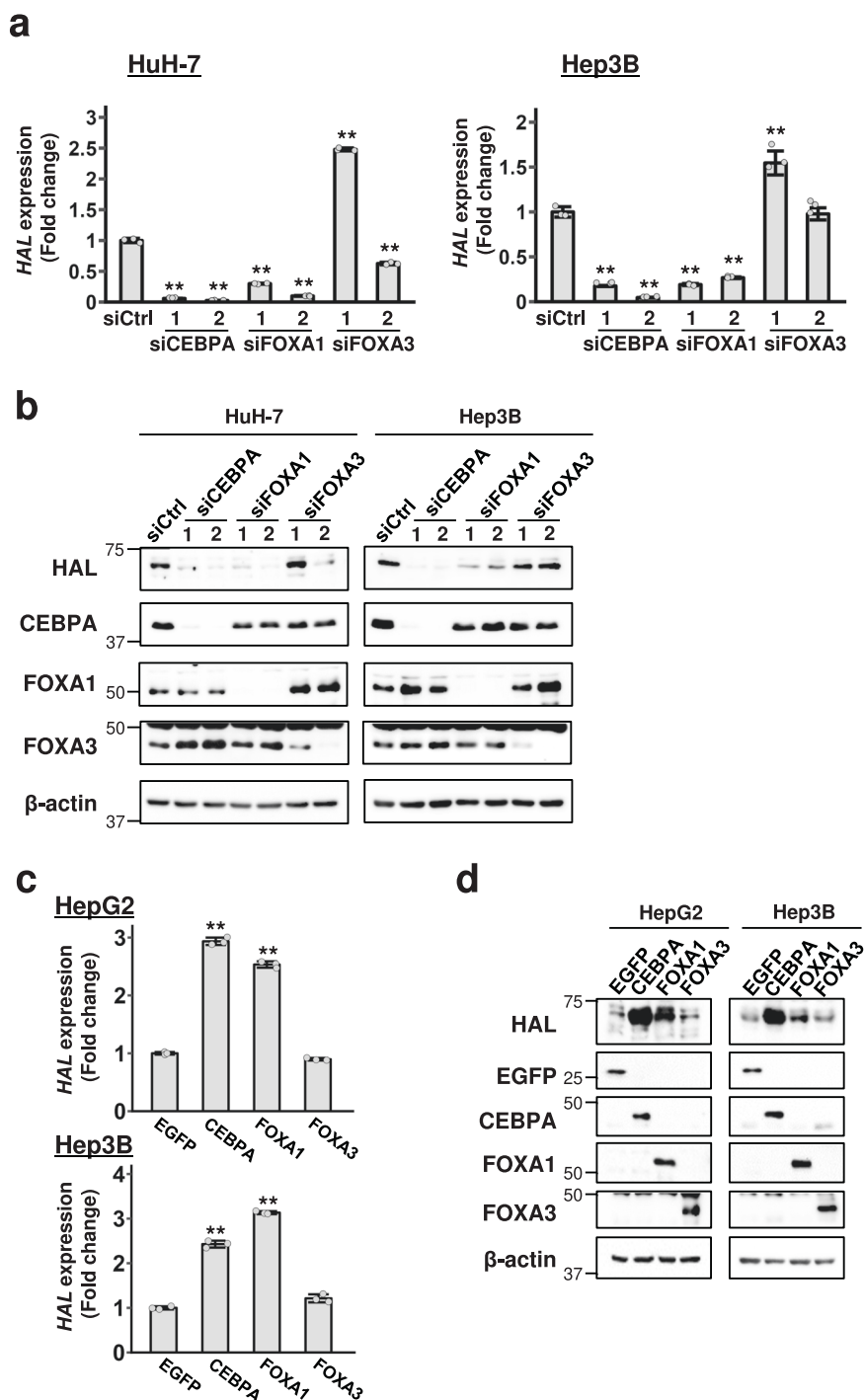


Fig. 1 | Identification of transcription factors that are negatively regulated by the β -catenin-TCF/LEF complex in liver cancer. **a** Hierarchical cluster analysis of HepG2 cells treated with siRNA targeting components of β -catenin-TCF/LEF complex. Expression levels of genes encoding candidate transcription factors, Wnt target genes (*AXIN2*, *LGR5*, *MYC*, and *RNF43*), and *HAL* are shown in the heatmap. The numbers after the gene symbols indicate the different microarray probes. Information of probe ID is shown in Supplementary Data 1c. **b** Expression levels of *CEBPA*, *FOXA1*, and *FOXA3* in HepG2 and HuH-6 cells treated with control, β -catenin (–9 and –10), or TCF7L2 siRNA were analyzed by RT-qPCR. The y-axis represents fold change of the expression in the cells treated with β -catenin or TCF7L2 siRNA compared to control siRNA. *HPRT1* was used as an internal control for qPCR. The data represent mean \pm SD from three-independent experiments. Statistical significance was determined by Dunnett’s test. $**p < 0.01$ vs siCtrl.

c Increased expression of *CEBPA*, *FOXA1*, and *FOXA3* by β -catenin or TCF7L2 siRNA in HepG2 cells. *AXIN2* was used as a direct target of the β -catenin/TCF complex. Since HepG2 cells carry a heterozygous deletion encompassing exon 3 and exon 4 of *CTNNB1*, immunoblot analysis of the cells depicted two bands corresponding to the wild-type (96 kDa) and mutant (75 kDa) β -catenin protein. **d** Effect of CHIR-99021, a GSK3 inhibitor, on the expression of β -catenin, *AXIN2*, *HAL*, *CEBPA*, *FOXA1*, and *FOXA3* in HuH-7 cells. **e** Expression of *HAL*, *CEBPA*, *FOXA1*, and *FOXA3* in hepatocellular carcinoma tissues with or without *CTNNB1* mutation. The expression values and genetic status of *CTNNB1* mutation were obtained from the dataset of 361 hepatocellular carcinoma (TCGA, Pan-Cancer Atlas). Statistical significance was determined by unpaired two-tailed *t*-test. Center line, median; Box limits, upper and lower quartiles; Whiskers, 1.5 \times interquartile range.

Fig. 3 | Involvement of CEBPA and FOXA1 in HAL expression. **a** Expression of *HAL* in HuH-7 and Hep3B cells treated with the indicated siRNAs. Expression was assessed by RT-qPCR. The y-axis represents the fold change in the expression of *HAL* observed in the cells treated with the indicated siRNAs compared to control siRNA. **b** Expression of *HAL*, *CEBPA*, *FOXA1*, and *FOXA3* in the cells treated with the indicated siRNAs was detected by immunoblotting. β -actin served as a loading control. **c** The effect of *CEBPA*, *FOXA1*, and *FOXA3* over-expression on the expression of *HAL* in HepG2 and Hep3B cells. Expression was assessed by RT-qPCR. The y-axis represents fold change in *HAL* expression observed in the cells over-expressing the indicated transcription factors relative to EGFP (control). **d** Expression of *HAL*, *CEBPA*, *FOXA1*, and *FOXA3* in the cells over-expressing the indicated plasmids was detected by immunoblotting. β -actin served as a loading control. Unless specified otherwise, data are represented as the mean \pm SD of three independent experiments. Statistical significance was determined by Dunnett's test. ** $p < 0.01$ vs siCtrl or EGFP.

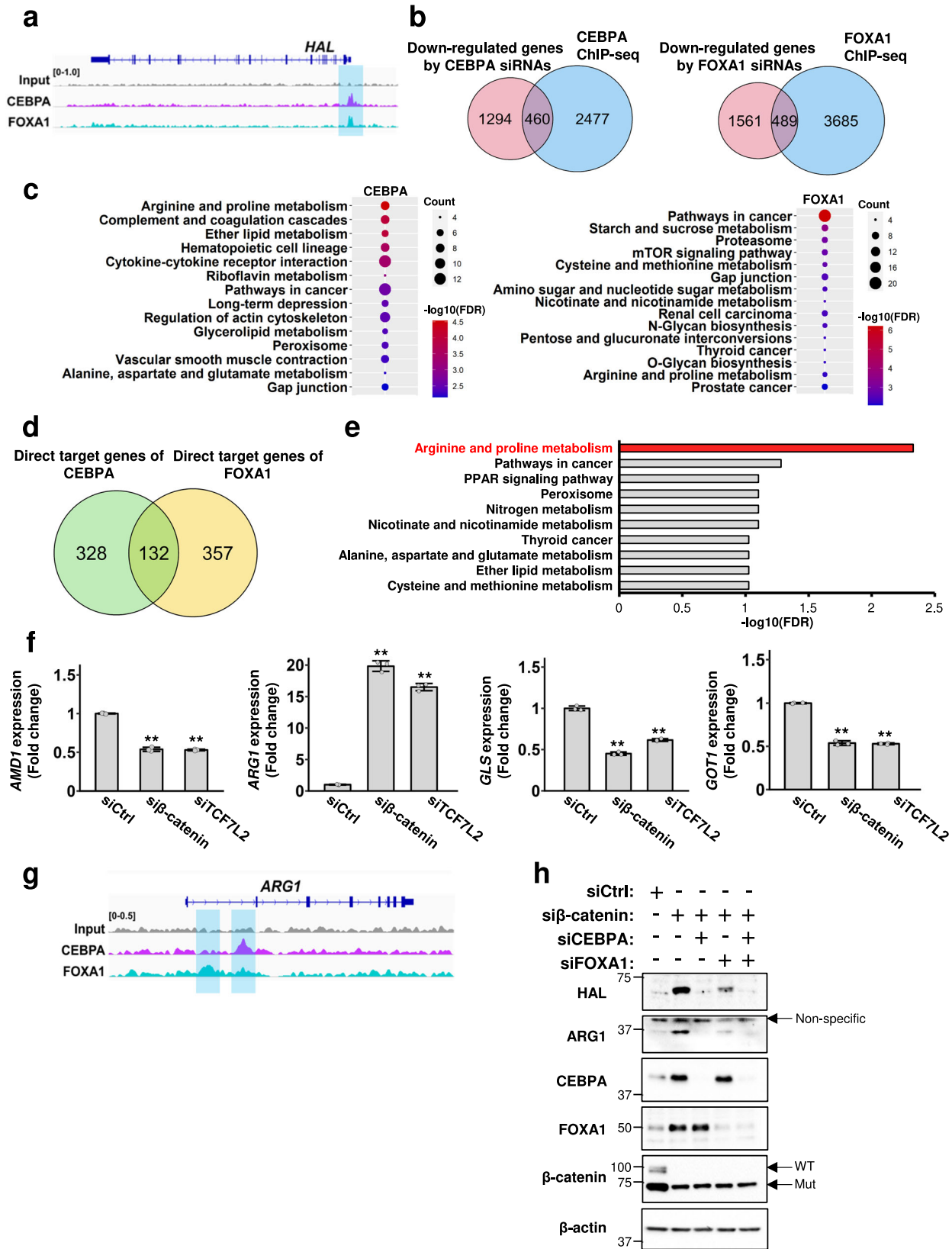


expression levels in HepG2 cells transfected with β -catenin with/without CEBPA or FOXA1 siRNA. As shown in Fig. 4h, knockdown of β -catenin alone increased the expression of CEBPA and FOXA1 as well as that of ARG1. Concomitant suppression of β -catenin and CEBPA or FOXA1 counteracted the induction of ARG1 by β -catenin siRNA. A similar result was obtained for HAL expression. These results suggest that Wnt signaling regulates the expression of HAL and ARG1 through CEBPA and FOXA1.

Wnt signaling pathway is associated with the levels of cellular amino acids

The down-regulation of *HAL* and *ARG1* by Wnt signaling is likely dependent on the type of tissue because the expression of *HAL* and *ARG1* did not decrease in the Wnt-activated colorectal adenocarcinoma (Supplementary

Fig. 6f). Since these enzymes are involved in the metabolism of histidine or arginine, we examined whether the levels of metabolites are regulated by the Wnt signaling pathway in liver cancer cells. Metabolome analysis was performed using capillary electrophoresis time-of-flight mass spectrometry and the levels of 116 metabolites were compared in the lysates from HepG2 cells transfected with control, β -catenin, or TCF7L2 siRNA. The heatmap depicted that metabolites commonly altered by both β -catenin and TCF7L2 siRNAs were mainly reduced (Fig. 5a and Supplementary Data 4a). Consistent with the increased expression of HAL and ARG1 by the siRNA, the levels of histidine and arginine were significantly decreased in the cells transfected with β -catenin or TCF7L2 siRNA (Fig. 5b). To determine whether the levels of these amino acids were regulated by CEBPA or FOXA1, we analyzed the levels of histidine and arginine in HepG2 cells



transfected with β-catenin siRNA in combination with CEBPA or FOXA1 siRNA (Supplementary Fig. 7a). As expected, the levels of histidine and arginine were significantly restored by the additional knockdown of CEBPA. There was also a trend toward restoration of histidine and arginine levels in cells treated with β-catenin and FOXA1 siRNAs. These results were

consistent with the western blotting results showing that knockdown of CEBPA and FOXA1 reduced the silencing effect of β-catenin on HAL and ARG1 expression (Fig. 4h). These findings further support the involvement of these transcription factors in cellular amino acid metabolism. Interestingly, inhibition of the Wnt signaling pathway significantly decreased a large

Fig. 4 | Gene set enrichment analysis using genes directly regulated by CEBPA and FOXA1 in liver cancer cells. **a** Visualization of ChIP-seq peaks of CEBPA (magenta) and FOXA1 (blue) in the genomic region of *HAL*. **b** Venn diagrams depicting the number of genes regulated by CEBPA and genes regulated by FOXA1 in HuH-7 cells. The overlapping genes were considered as direct targets of each transcription factor. **c** Over-representation analysis (ORA) using KEGG pathway gene sets with the 460 and 489 genes directly regulated by CEBPA and FOXA1, respectively. Significant pathways are shown with *q*-value and the number of genes. **d** Venn diagram showing common direct targets of CEBPA and FOXA1. **e** ORA

using the 132 common target genes (FDR *q*-value < 0.01). **f** The expression levels of *AMD1*, *ARG1*, *GLS*, and *GOT1* in HepG2 cells treated with β -catenin or TCF7L2 siRNA analyzed by RT-qPCR. *HPRT1* was used as an internal control. Data are represented as the mean \pm SD of three independent experiments. Statistical significance was determined by Dunnett's test. $^{**}p < 0.01$ vs siCtrl. **g** Visualization of ChIP-seq peaks of CEBPA (magenta) and FOXA1 (blue) in the genomic region of *ARG1*. **h** Expression of *HAL* and *ARG1* in HepG2 cells treated with CEBPA and/or FOXA1 siRNA in combination with β -catenin siRNA.

number of amino acids, resulting in the suppression of total levels of amino acids (Supplementary Fig. 7b). In addition, we found that the suppression of the pathway decreased the levels of lactic acid and increased that of acetyl-CoA (Fig. 5c), implying that the inhibition of the Wnt signaling pathway may suppress the Warburg effect in liver cancer cells.

Subsequently, we performed pathway analysis using the data of 41 metabolites that were significantly regulated by β -catenin and TCF7L2 siRNA, and identified the enrichment of 13 metabolite sets (FDR *q*-values < 0.01, Fig. 5d and Supplementary Data 4b). Consistent with the change in the level of arginine, "Arginine and Proline Metabolism" was in the list of the 13 metabolite sets. It is of note that "Urea cycle" was listed as the most significant metabolite set. This result suggests that the activated Wnt signaling pathway may regulate the urea cycle through down-regulation of *ARG1* in hepatoma cells because *ARG1* encodes the focal enzyme of the urea cycle hydrolyzing L-arginine to urea and L-ornithine. We further investigated whether other genes in the urea cycle were modulated by the Wnt signaling pathway using the microarray data (Supplementary Data 1b). In addition to *ARG1*, ornithine transcarbamylase (*OTC*) expression was remarkably increased by the knockdown of β -catenin and TCF7L2 (Fig. 5e), and argininosuccinate synthase 1 (*ASS1*) and argininosuccinate lyase (*ASL*) expression was also substantially increased by the knockdown. These results suggest that the metabolism of amino acids and the urea cycle are altered by the activated Wnt/ β -catenin signaling pathway and that these changes may contribute to the development and progression of liver cancer cells.

Discussion

In this study, we have shown that the promoter region of *HAL* was transcriptionally regulated by transcription factors CEBPA and FOXA1, and that the two were down-regulated by the Wnt signaling pathway in the liver cancer cells. In addition, we have uncovered that the pathway modulates intracellular metabolites at least in part by *HAL* and *ARG1* through suppression of CEBPA and FOXA1.

It was previously reported that *HAL* expression was significantly decreased in the liver of *Hnf4a* (hepatocyte nuclear factor 4 α)-knockout mice²⁰. In addition, over-expression of β -catenin decreased the expression of *HNF4A* in Hep3B cells²¹. These data led us to additionally investigate whether HNF4A regulates *HAL* in the same manner as CEBPA and FOXA1. The knockdown of β -catenin and TCF7L2 increased the expression of *HNF4A* (Supplementary Fig. 1d). Although knockdown of HNF4A significantly decreased the expression of *HAL* (Supplementary Fig. 1e), it did not affect the reporter activity of the *HAL* promoter (Supplementary Fig. 1f). Therefore, *HAL* expression is regulated by at least three transcription factors, CEBPA, FOXA1, and HNF4A in liver cells, and CEBPA and FOXA1 function through the interaction with the proximal promoter region of *HAL*.

FOXA1 or hepatocyte nuclear factor 3 α (HNF3A), a liver-enriched transcription factor, was reported to decrease the transcription of *PIK3R1*, and suppress the viability and motility of HCC cells through the inhibition of PI3K-Akt signaling²². In addition, FOXA1 positively regulates miR-122 that is specifically suppressed in liver tumors with poor prognosis²³. These reports suggest that FOXA1 may function as a tumor suppressor in HCC, and their results are consistent with our finding that the expression of FOXA1 was suppressed in liver cancer cells with activated Wnt signaling. In our reporter gene assay, overexpression or suppression of FOXA1 had limited effect on the activity of the *HAL* promoter (Fig. 2), but the expression

levels of *HAL* were dependent on FOXA1 expression (Fig. 3). This discrepancy may be explained by the fact that FOXA1 is a pioneer factor, which recognizes specific DNA sequences exposed on the surface of a nucleosome and allows other transcription factors and histone modifiers to access silent genes that are inaccessible to general transcription factors^{24,25}. Our results indicated that alteration of chromatin structure by FOXA1 might be essential for the regulation of the transcription of *HAL*. Alternatively, a regulatory region other than -90 and -44 bp may be involved in the regulation of *HAL* transcription.

Microarray expression analysis of HepG2 cells with β -catenin or TCF/LEF siRNA confirmed that known Wnt target genes including *MYC*, *RNF43*, *AXIN2*, and *LGR5* were listed as down-regulated genes (Fig. 1a). Several members of FOX-family transcription factors such as *FOXD1* and *FOXP1* were also similarly reduced by these siRNAs, suggesting that *FOXD1* and *FOXP1* may be targets of the canonical Wnt signaling pathway. It is of note that *FOXD1* is aberrantly overexpressed in colorectal cancer, and it promotes the progression of cancer through the activation of the ERK1/2 signaling pathway²⁶. Regarding *FOXP1*, it has a paradoxical role in tumorigenesis, depending on the type of cancer²⁷. Both *FOXD1* and *FOXP1* have been reported as activators of Wnt/ β -catenin signaling in prostate cancer and diffuse large B cell lymphoma, respectively^{28,29}. Therefore, these factors may mediate a positive feedback loop in the Wnt signaling pathway and accelerate the progression of Wnt-driven cancer. The role of these factors in liver carcinogenesis needs to be clarified in future studies.

CEBPA is a transcription factor that is abundantly expressed in the liver, skin, mammary gland, and adipose tissue (GTEx Portal; <https://gtexportal.org/home/>). The repression of CEBPA was shown in a wide range of liver pathologies including liver fibrosis³⁰ and cirrhosis³¹. It has been reported that the suppression of CEBPA was caused by the activation of Wnt signaling in mouse embryonic fibroblasts³² and liver cancer cells³³ at the protein levels. Reportedly, CEBPA protein was degraded by the interaction with tribbles homolog 2 (TRIB2) and constitutive photomorphogenesis 1 (COP1)³⁴ or tripartite motif-containing protein 21 (TRIM21)³⁵, and TRIB2 was induced by activation of Wnt/TCF signaling³³. However, we showed in this study that *CEBPA* was transcriptionally reduced by the activation of Wnt signaling. Because the expression of *FOXA1* and *CEBPA* was not induced by the knockdown of β -catenin in colorectal cancer cells, transcription factors that are expressed in liver tissues might be involved in the regulation of *CEBPA* and/or *FOXA1* expression.

HAL and *ARG1*, the two liver-specific Wnt target genes, encode enzymes associated with amino acid metabolisms. *HAL* catalyzes the first reaction in histidine catabolism³⁶. Reportedly, inhibition of the components of the histidine degradation pathway such as *HAL* and *AMDHD1* (amido-hydrolyase domain containing 1) induces the levels of tetrahydrofolate, which decreases the sensitivity of hematopoietic cancer cells to methotrexate⁸. In addition, the sensitivity to methotrexate in lung cancer cells was decreased by the knockout of *HAL*⁸. These data suggest a link between chemoresistance of the cells and Wnt-activation. Therefore, the Wnt/ β -catenin pathway may be involved in chemoresistance and cell differentiation through the suppression of histidine catabolism in hepatoma cells. As for *ARG1*, which is abundantly expressed in the liver, it cleaves arginine to urea and ornithine in the urea cycle³⁷. In this study, we showed that suppressed Wnt signaling changed the levels of metabolites as well as genes associated with the urea cycle (Fig. 5d, e). In agreement with our data, proteomics analysis of liver-specific *Apc* knockout mice demonstrated that

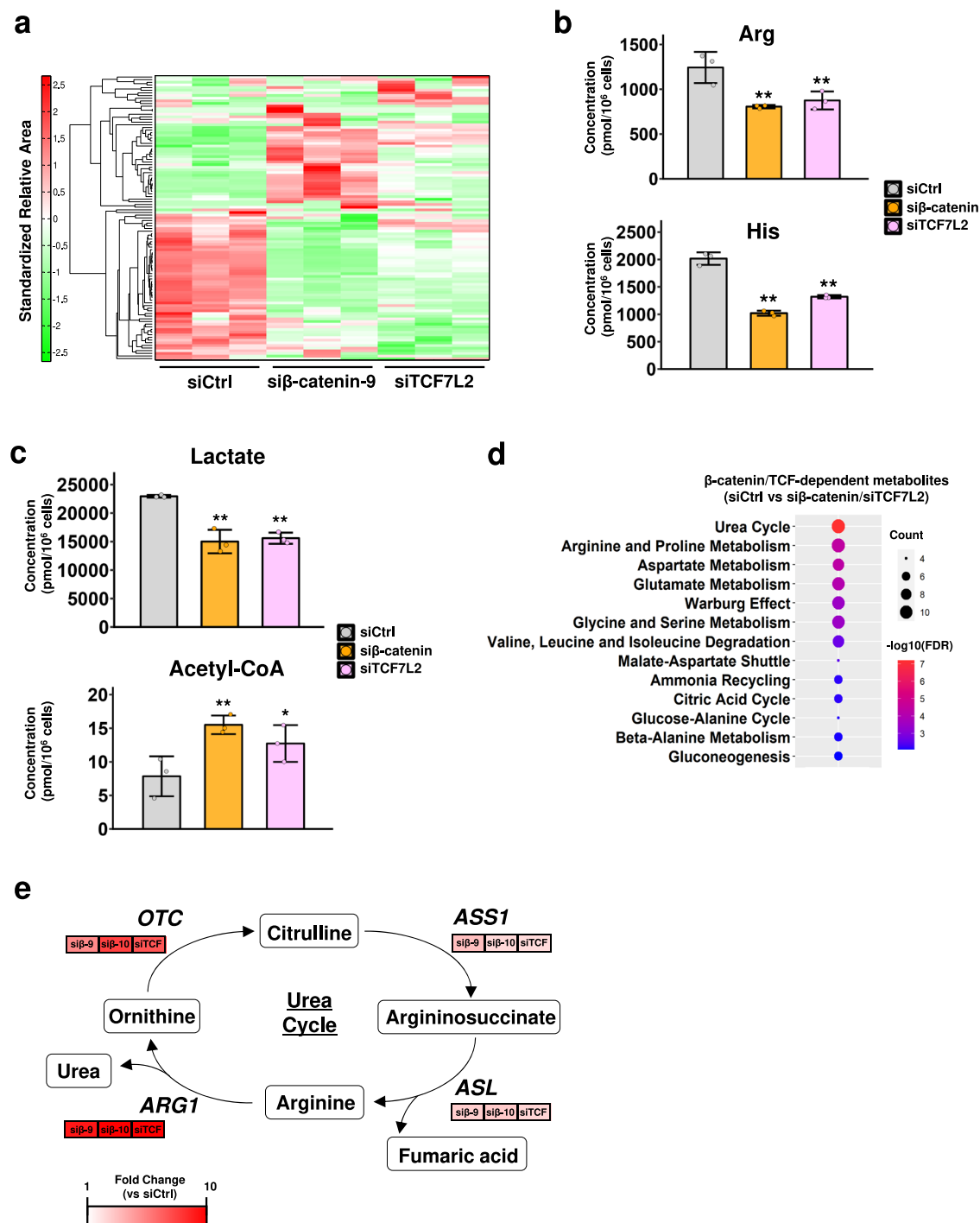


Fig. 5 | Alterations in the levels of amino acids in β-catenin- or TCF7L2-depleted cells. **a** Metabolite analysis using HepG2 cells treated with control, β-catenin, or TCF7L2 siRNA. Each group was analyzed in triplicate. **b, c** Quantitative analysis of the indicated metabolites using mass spectrometry in the HepG2 cells treated with control, β-catenin, or TCF7L2 siRNA. The y-axis represents the concentration (pmol/10⁶ cells) of metabolites. **b** Levels of arginine and histidine. **c** Levels of lactate and acetyl-CoA. **d** Metabolic pathway analysis using metabolites that were commonly altered by the knockdown of β-catenin and TCF7L2. FDR *q*-value < 0.01 was considered significant.

e A simplified schematic representation of the urea cycle and related enzymes. ASS1, argininosuccinate synthetase1; ASL, argininosuccinate lyase; OTC, ornithine transcarbamylase. The microarray data (Fig. 1a) were used to generate altered expression values of OTC, ARG1, ASS1, and ASL (fold change) in the cells treated with β-catenin (siβ-9 and siβ-10) or TCF7L2 (siTCF) siRNA compared to control siRNA. Unless specified otherwise, data are represented as the mean ± SD of three independent cultures. Statistical significance was determined by Dunnett's test. **p* < 0.05, ***p* < 0.01 vs siCtrl.

the most differentially expressed proteins were related to a metabolic pathway, and that the expression of Arg1 and Cps1, urea cycle related enzymes, were suppressed in the knockout mice³⁸. Therefore, activated Wnt signaling may accumulate intracellular ammonia by suppression of the urea cycle in liver cancer. The suppression may help the synthesis of various

proteins necessary to produce new daughter cells by decreasing the degradation of amino acids³⁹. Indeed, our results indicated that suppression of the signaling caused the reduction in the total amount of amino acids (Supplementary Fig. 7b), which may be due to the acceleration of the urea cycle and degradation of amino acids (Fig. 5e). Importantly, it has been reported

that the dysregulation of the urea cycle is widely observed in liver tumors and profoundly affects carcinogenesis, mutagenesis, and immunotherapy response⁴⁰. Targeting the urea cycle might be an attractive therapeutic strategy for patients with liver tumor driven by the activated Wnt pathway.

As shown in Fig. 5c, we observed reduced glycolysis by β -catenin or TCF7L2 siRNAs in HepG2 cells, suggesting that Wnt signaling is associated with glycolysis. It has been reported that Wnt signaling up-regulates pyruvate dehydrogenase kinase-1 (PDK1) in colorectal cancer cells, leading to the enhanced glycolysis through the inhibition of pyruvate dehydrogenase (PDH) activity⁴¹. Consistent with this report, we confirmed that the expression of *PDK1* was also decreased by the suppression of Wnt signaling in HepG2 cells (Supplementary Data 1b), corroborating that PDK1 plays a pivotal role in glycolysis as a downstream of the Wnt signaling in liver tissue. In cancer cells, increased catabolism of glucose (Warburg effect) anaerobically rather than aerobically leads increased glucose uptake and lactic acid production⁴¹. It is noteworthy that increased levels of lactic acid by enhanced glycolysis promote immune evasion in tumors^{42,43}. Therefore, the activation of the Wnt/ β -catenin signaling pathway may, in part, suppress anti-tumor immunity by increased lactic acid production⁴⁴.

In conclusion, we identified two transcription factors, CEBPA and FOXA1, enriched in the liver as cellular context-dependent targets of the Wnt signaling. Our findings will provide insights into the relationship between liver metabolism and the Wnt signaling pathway. Further investigations of tissue-specific Wnt targets may uncover a role of the pathway involved in human carcinogenesis.

Methods

Cell culture

Human hepatoma cells, HepG2 and Hep3B, were obtained from the American Type Culture Collection (ATCC, Manassas, VA), and HuH-6 and HuH-7 cells were obtained from the Japanese Collection of Research Bioresources Cell Bank (JCRB, Osaka, Japan). These cells were confirmed to be mycoplasma-free and authenticated by Hoechst DNA staining and short tandem repeat profiling, respectively (ATCC and JCRB). Retrovirus packaging cells PLAT-A were provided from Dr. Toshio Kitamura (The University of Tokyo). All cells were grown in appropriate media containing 10% fetal bovine serum (Biosera, Nuaille, France) and 1% penicillin/streptomycin solution (Fujifilm Wako Pure Chemical, Osaka, Japan). The PLAT-A cells were maintained in complete medium supplemented with puromycin (1 μ g/ml, Merck, Darmstadt, Germany) and blasticidin (10 μ g/ml, Fujifilm Wako Pure Chemical).

Expression plasmids

The entire coding region of *FOXA1*, *FOXA3*, and *HNF4A* were amplified by RT-PCR (KOD One, Toyobo, Osaka, Japan) using human liver cDNA as template. The coding region of *CEBPA* was amplified using MSCV-*CEBPA* plasmid (a kind gift from Dr. Atsushi Iwama, The University of Tokyo). The PCR products were cloned into pCMV-Myc-N vector (Takara Bio, Shiga, Japan). The primer sequences used for the amplification are listed in Supplementary Data 5a. The cloned DNA fragments in the plasmids were confirmed by Sanger sequencing (3500xL GeneticAnalyzer, Thermo Fisher Scientific, Waltham, MA).

Gene silencing

Two independent siRNAs targeting each gene were used for gene silencing. *CEBPA*, *FOXA1*, *FOXA3*, and *HNF4A* siRNAs were purchased from Integrated DNA Technologies (Coralville, IA). β -catenin, *LEF1*, *TCF7*, *TCF7L1*, and *TCF7L2* siRNAs were obtained from Merck. Control siRNA (ON-TARGETplus Non-targeting Pool) was purchased from Horizon Discovery (Cambridge, UK). The target sequences of the siRNAs are shown in Supplementary Data 5b. Cells were transfected with the siRNAs (10 nM) for 48 h using Lipofectamine RNAiMAX (Thermo Fisher Scientific). The gene-silencing efficiency of each siRNA was confirmed by quantitative RT-PCR (qRT-PCR) or immunoblotting.

Quantitative PCR

Total RNA was isolated from cultured cells using RNeasy Mini Kit (Qiagen, Valencia, CA). cDNA was synthesized from 1 μ g of total RNA using ReverTraAce (Toyobo). qPCR was performed using KAPA SYBR Fast qPCR Kit (Kapa Biosystems, Wilmington, MA) and StepOnePlus (Thermo Fisher Scientific) with sets of primers listed in Supplementary Data 5a. The levels of transcripts were determined using the relative standard curve method, and hypoxanthine phosphoribosyl transferase 1 (*HPRT1*) was used as an internal control.

Immunoblotting

Cells were lysed in radioimmunoprecipitation assay buffer (50 mM Tris-HCl, pH 8.0, 150 mM NaCl, 0.5% sodium deoxycholate, 1% Nonidet P-40, 0.1% sodium dodecyl sulfate) supplemented with a Protease Inhibitor Cocktail Set III (Merck). The proteins were separated by SDS-PAGE and transferred to a nitrocellulose membrane (Cytiva, Marlborough, MA). After blocking with 5% skim milk powder in TBS-T (Tris-buffered saline-Tween20), the membranes were incubated with anti-HAL (Merck, Cat# HPA038547, 1:1000), anti- β -catenin (Cell Signaling Technology, Danvers, MA, Cat# 9582, 1:1000), anti-TCF7L2 (Merck, Cat#05-511, 1:1000), anti-AXIN2 (Cell Signaling Technology, Cat# 2151, 1:1000), anti-CEBPA (Thermo Fisher Scientific, Cat# PA5-77911, 1:1000), anti-FOXA1 (Merck, Cat# 17-10267, 1:1000 and Santa Cruz Biotechnology, Santa Cruz, CA, Cat# sc-101058, 1:1000), anti-FOXA3 (Abcam, Cambridge, UK, Cat# ab108454, 1:1000), anti-ARG1 (Santa Cruz Biotechnology, Cat# sc-365547, 1:1000), anti-GFP (Santa Cruz Biotechnology, Cat# sc-9996, 1:1000), or anti- β -actin (Merck, Cat# A5441, 1:2500) antibody overnight at 4 °C. Horseradish peroxidase-conjugated anti-mouse (NA931V, Cytiva), anti-rabbit IgG (NA9340V, Cytiva), or VeriBlot for IP Detection Reagent (HRP) (ab131366, Abcam) served as the secondary antibody. The membranes were incubated with ImmunoStar LD (Fujifilm Wako Pure Chemical) or SuperSignal West Pico Chemiluminescent Substrate (Thermo Fisher Scientific), and the chemiluminescence images were captured using Amersham Imager 600 system (Cytiva) or ChemiDoc XRS+ System (Bio-rad, Hercules, CA). β -actin was used as a loading control. Probing with a loading control was performed in parallel with the target antibody by cutting the membrane prior to antibody incubation.

Site-directed mutagenesis

Putative FOX and/or CEBP transcription factor binding motifs in the 5'-flanking region of the *HAL* gene (pHAL -90/+147) were mutated by site-directed mutagenesis⁷. The 5'-flanking region of *HAL*, between -90 bp and +147 bp, was amplified using KOD-Plus-Neo (Toyobo) with each primer set (Supplementary Data 5a). The PCR products were digested with *Dpn* I (Takara Bio) for 2 h at 37 °C, followed by transformation into *E. coli*. Successful mutagenesis was confirmed by Sanger sequencing.

Treatment with GSK-3 α / β inhibitor

A GSK-3 α / β inhibitor, CHIR-99021, was purchased from MedChemExpress (Monmouth Junction, NJ), and dissolved in dimethyl sulfoxide (DMSO). HuH-7 cells were treated with CHIR-99021 (5 μ M) or DMSO for 24 h.

Luciferase reporter assays

HepG2 and Hep3B cells seeded on 12-well plates were transfected with 0.25 μ g of reporter plasmids and 0.05 μ g of pRL-null (Promega, Madison, WI) in combination with the indicated siRNAs using Lipofectamine 2000 reagent (Thermo Fisher Scientific). After 48 h, the cells were harvested, and reporter activity was measured by dual luciferase assay system (TOYO B-Net, Tokyo, Japan). To examine the effect of FOXA1, FOXA3, and CEBPA on the activity of *HAL* promoter, HepG2 cells were co-transfected with *HAL* reporter plasmid (0.2 μ g) and pRL-null plasmid (0.05 μ g) in combination with plasmids expressing FOXA1 (0.2 μ g), FOXA3 (0.2 μ g), or CEBPA (0.02 μ g) using FuGENE6 reagent (Promega). Firefly luciferase activity was normalized to *Renilla* luciferase activity (pRL-null).

Retroviral transduction

CEBPA, *FOXA1*, and *FOXA3* were sub-cloned into pMXs-Puro retroviral vector (a kind gift from Dr Kitamura, The University of Tokyo) by the Gibson Assembly cloning method (NEBuilder HiFi DNA Assembly Master Mix, New England Biolabs, Ipswich, MA). The sequences of primers used for the amplification are shown in Supplementary Data 5a. For production of retroviral particles, PLAT-A packaging cells were transfected with pMXs-EGFP (enhanced green fluorescent protein), pMXs-CEBPA, pMXs-FOXA1, or pMXs-FOXA3 for 24 h. After changing the medium, the cells were further incubated for 24 h, and supernatants containing the retrovirus were collected and used for infection. Forty-eight hours after infection, HepG2 cells were selected in the medium containing 1.625 µg/ml of puromycin, and Hep3B and HuH-7 cells were selected with 2.5 µg/ml of puromycin.

Microarray analysis

Total RNA was isolated from HepG2 cells treated with β-catenin, TCF7, TCF7L1, TCF7L2, or LEF1 siRNA (10 nM) for 48 h using Lipofectamine RNAiMAX. Total RNA was extracted using the RNeasy Plus Mini kit (Qiagen), and subsequently expression profiles were analyzed by SurePrint G3 Gene Expression 8 × 60K microarray (Agilent Technologies, Santa Clara, CA) according to the manufacturer's protocol. Data processing and unsupervised hierarchical clustering were performed using GeneSpring GX14.1 software (Agilent Technologies). In hierarchical clustering, Pearson's center and centroid linkage were used as distance metric and linkage function, respectively.

RNA-seq analysis

HuH-7 cells were transfected with control, FOXA1, or CEBPA siRNAs (10 nM) for 48 h. Total RNA was extracted from the cells using the RNeasy Plus Mini kit. Agilent Bioanalyzer device (Agilent Technologies) was used to assess the quality of extracted RNA. Subsequently, RNA-seq libraries were prepared with total RNA (100 ng) using an NEBNext Ultra II Directional RNA Library Prep Kit (New England Biolabs) according to the manufacturer's protocol. The libraries were sequenced with 100 bp paired-end reads on the DNBSEQ-G400RS (MGI Tech, Shenzhen, China). The analysis of sequencing data was performed by a standard RNA-seq analytical pipeline. Briefly, STAR(v2.7.3a)⁴⁵ was used to align the sequencing data to the human genome (hg38). Quantification of gene expression was performed using RSEM (v1.3.3)⁴⁶. The DESeq2 package (v1.26.0)⁴⁷ was used to normalize the read count data and test for differential gene expression.

Chromatin immunoprecipitation followed by high-throughput sequencing (ChIP-seq)

ChIP-seq was performed using anti-CEBPA (Thermo Fisher Scientific, Cat# PA5-77911) or anti-FOXA1 antibody (Merck, Cat# 17-10267)⁴⁸. HuH-7 cells were cross-linked with 1% formaldehyde for 10 min at room temperature, and 0.1 M glycine was added to quench the formaldehyde. Chromatin extracts were sheared by micrococcal nuclease digestion (New England Biolabs), and protein-DNA complexes were immunoprecipitated with 5 µg of anti-CEBPA or anti-FOXA1 antibody bound to Dynabeads Protein G (Thermo Fisher Scientific). Normal rabbit IgG (Santa Cruz Biotechnology) was used as a negative control. Decrosslinking was performed at 65 °C overnight, and samples were subsequently treated with RNase A (Merck) for 2 h at 37 °C and Proteinase K (Merck) for 30 min at 55 °C. The precipitated protein-DNA complexes were purified by the conventional DNA extraction method, and the purified DNA was used for preparation of sequence libraries. Concentration of input and ChIP'd DNA was measured using Qubit dsDNA HS Assay kit (Thermo Fisher Scientific). ChIP-seq libraries were prepared with 1 ng of DNA using an NEBNext Ultra II DNA Library Prep kit (New England Biolabs) according to the manufacturer's protocol. The libraries were sequenced with 150 bp paired-end reads on the DNBSEQ-G400RS. The sequencing data were aligned to human genome (GRCh38) using Bowtie2 (v2.4.1)⁴⁹. Peak calling followed by assignment

of peaks to genes was performed using MACS2 (v3.6)⁵⁰ and HOMER (v4.11)⁵¹. Peaks with q -value < 0.05 were considered significant.

To validate the results of ChIP-seq analysis, ChIP followed by quantitative PCR (ChIP-qPCR) was performed using KAPA SYBR Fast qPCR Kit (Kapa Biosystems) and StepOnePlus (Thermo Fisher Scientific)⁵². The precipitated DNAs were subjected to qPCR analysis using sets of primers encompassing genomic regions with peaks. As negative control non-immune IgG and control primers to amplify exon 1 of the glyceraldehyde-3-phosphate dehydrogenase (*GAPDH*) were used. The primer sequences used are listed in Supplementary Data 5a.

Metabolite extraction and analysis

After aspiration of culture medium, the cells were washed twice with 5% mannitol solution, and incubated with methanol at room temperature for 30 s to suppress enzyme activity. Next, internal standards (H3304-1002, Human Metabolome Technologies, Yamagata, Japan) were added to the cell extract, followed by further incubation at room temperature for 30 s. The cell extract was then centrifuged at 2300 × g , 4 °C for 5 min, after which the supernatant was centrifugally filtered through a Millipore 5-kDa cutoff filter (UltrafreeMC-PLHCC, Human Metabolome Technologies) at 9100 × g , 4 °C for 5 h to remove macromolecules. Subsequently, the filtrate was evaporated to dryness under vacuum and reconstituted in Milli-Q water for metabolome analysis at Human Metabolome Technologies.

Metabolome analysis was conducted according to the C-SCOPE package (Human Metabolome Technologies), using capillary electrophoresis time-of-flight mass spectrometry (CE-TOFMS) for cation analysis and CE-tandem mass spectrometry (CE-MS/MS) for anion analysis based on the methods described previously^{53,54}. Peaks were extracted using MasterHands, automatic integration software (Keio University, Yamagata, Japan)⁵⁵ and MassHunter Quantitative Analysis B.04.00 (Agilent Technologies) in order to obtain peak information including m/z , peak area, and migration time (MT). Signal peaks were annotated according to the metabolite database of Human Metabolome Technologies, based on their m/z values and MTs. The peak area of each metabolite was normalized to internal standards, and metabolite concentration was evaluated by standard curves with three-point calibrations using each standard compound. Hierarchical cluster analysis⁵⁶ was performed by Human Metabolome Technologies's proprietary MATLAB and R programs, respectively. Detected metabolites were plotted on metabolic pathway maps using VANTED software⁵⁷.

Over-representation analysis (ORA)

The biological significance of the expression and metabolome data was assessed by over-representation analysis. Differentially expressed genes by either CEBPA or FOXA1 siRNAs were subjected to KEGG pathway analysis. Gene sets with FDR q -value < 0.01 were considered significant. MetaboAnalyst⁵⁸ was used for the analysis of differential levels of metabolites by β-catenin and TCF7L2 siRNA. Metabolite sets with FDR q -value < 0.01 were considered significant.

Statistics and reproducibility

The unpaired two-tailed t -test was used when two independent groups were compared. For groups larger than two, statistical analysis was performed using one-way analysis of variance (ANOVA) with Dunnett's post hoc test. These statistical analyses were performed using the Bell-Curve for Excel software (Social Survey Research Information, Tokyo, Japan). A p -value < 0.05 was considered statistically significant. Sample sizes are indicated in the figure legends. Data are displayed with error bars showing mean ± SD and individual samples in a bar graph. In RNA-seq and ChIP-seq analyses, significance level was set at a Benjamini-Hochberg FDR-adjusted p -value (i.e., q -value) of less than 0.05.

Reporting summary

Further information on research design is available in the Nature Portfolio Reporting Summary linked to this article.

Data availability

Microarray (GSE244527), RNA-seq (GSE244526), and ChIP-seq (GSE244525) data generated in this study were deposited in the Gene Expression Omnibus (GEO) database. Plasmids generated in this study were deposited into Addgene (pCMV-Myc-CEBPA: 219393, pCMV-Myc-FOXA1: 219394, pCMV-Myc-FOXA3: 219395, pCMV-Myc-HNF4A: 219399). All data supporting the findings of this study are available within the paper, its Supplementary Figs., and Supplementary Data. The source data for the graphs in this study are provided in Supplementary Data 5c–g. All uncropped blots are provided in Supplementary Figs. 8–16.

Received: 4 November 2023; Accepted: 16 April 2024

Published online: 29 April 2024

References

- Sanchez-Vega, F. et al. Oncogenic signaling pathways in the Cancer Genome Atlas. *Cell* **173**, 321–337.e10 (2018).
- Muzny, D. M. et al. Comprehensive molecular characterization of human colon and rectal cancer. *Nature* **487**, 330–337 (2012).
- Totoki, Y. et al. Trans-ancestry mutational landscape of hepatocellular carcinoma genomes. *Nat. Genetics* **46**, 1267–1273 (2014).
- Sansom, O. J. et al. Myc deletion rescues Apc deficiency in the small intestine. *Nature* **446**, 676–679 (2007).
- Tetsu, O. & McCormick, F. Beta-catenin regulates expression of cyclin D1 in colon carcinoma cells. *Nature* **398**, 422–426 (1999).
- Ohsugi, T. et al. Anti-apoptotic effect by the suppression of IRF1 as a downstream of Wnt/ β -catenin signaling in colorectal cancer cells. *Oncogene* **38**, 6051–6064 (2019).
- Yamaguchi, K. et al. Bidirectional reporter assay using HAL promoter and TOPFLASH improves specificity in high-throughput screening of Wnt inhibitors. *Biotechnol. Bioeng.* **114**, 2868–2882 (2017).
- Kanarek, N. et al. Histidine catabolism is a major determinant of methotrexate sensitivity. *Nature* **559**, 632–636 (2018).
- De La, M., Sarasola, P., Delgado, M. A. T. & Nicoud, M. B. Histamine in cancer immunology and immunotherapy. Current status and new perspectives. *Pharmacol. Res. Perspect.* **9**, 27 (2021).
- Dang, C. V., Le, A. & Gao, P. MYC-induced cancer cell energy metabolism and therapeutic opportunities. *Clin. Cancer Res.* **15**, 6479–6483 (2009).
- Pate, K. T. et al. Wnt signaling directs a metabolic program of glycolysis and angiogenesis in colon cancer. *EMBO J.* **33**, 1454–1473 (2014).
- Sprowl-Tanio, S. et al. Lactate/pyruvate transporter MCT-1 is a direct Wnt target that confers sensitivity to 3-bromopyruvate in colon cancer. *Cancer Metab.* **4**, 20 (2016).
- Lee, S. Y. et al. Wnt/snail signaling regulates cytochrome c oxidase and glucose metabolism. *Cancer Res.* **72**, 3607–3617 (2012).
- Sherwood, V. WNT signaling: an emerging mediator of cancer cell metabolism? *Mol. Cell Biol.* **35**, 2–10 (2015).
- Oginuma, M. et al. A gradient of glycolytic activity coordinates FGF and Wnt signaling during elongation of the body axis in amniote embryos. *Dev. Cell* **40**, 342–353.e10 (2017).
- Laissue, P. et al. Association of FOXD1 variants with adverse pregnancy outcomes in mice and humans. *Open Biol.* **6**, 160109 (2016).
- Shu, W., Yang, H., Zhang, L., Lu, M. M. & Morrissey, E. E. Characterization of a new subfamily of winged-helix/forkhead (Fox) genes that are expressed in the lung and act as transcriptional repressors. *J. Biol. Chem.* **276**, 27488–27497 (2001).
- Li, S., Weidenfeld, J. & Morrissey, E. E. Transcriptional and DNA binding activity of the Foxp1/2/4 family is modulated by heterotypic and homotypic protein interactions. *Mol. Cell Biol.* **24**, 809–822 (2004).
- Schrem, H., Jü, J., Klempnauer, J. & Borlak, J. Liver-enriched transcription factors in liver function and development. Part I: the hepatocyte nuclear factor network and liver-specific gene expression. *Pharmacol. Rev.* **54**, 129–158 (2002).
- Gougelet, A. et al. T-cell factor 4 and β -catenin chromatin occupancies pattern zonal liver metabolism in mice. *Hepatology* **59**, 2344–2357 (2014).
- Yang, M. et al. A double-negative feedback loop between Wnt- β -catenin signaling and HNF4 α regulates epithelial-mesenchymal transition in hepatocellular carcinoma. *J. Cell. Sci.* **126**, 5692–5703 (2013).
- He, S., Zhang, J., Zhang, W., Chen, F. & Luo, R. FOXA1 inhibits hepatocellular carcinoma progression by suppressing PIK3R1 expression in male patients. *J. Exp. Clin. Cancer Res.* **36**, 175 (2017).
- Coulouarn, C., Factor, V. M., Andersen, J. B., Durkin, M. E. & Thorgeirsson, S. S. Loss of miR-122 expression in liver cancer correlates with suppression of the hepatic phenotype and gain of metastatic properties. *Oncogene* **28**, 3526 (2009).
- Cirillo, L. A. et al. Opening of compacted chromatin by early developmental transcription factors HNF3 (FoxA) and GATA-4. *Mol. Cell* **9**, 279–289 (2002).
- Balsalobre, A. & Drouin, J. Pioneer factors as master regulators of the epigenome and cell fate. *Nat. Rev. Mol. Cell Biol.* **23**, 449–464 (2022).
- Pan, F., Li, M. & Chen, W. Original article FOXD1 predicts prognosis of colorectal cancer patients and promotes colorectal cancer progression via the ERK 1/2 pathway. *Am. J. Transl. Res.* **10**, 1522–1530 (2018).
- Koon, H. B., Ippolito, G. C., Banham, A. H. & Tucker, P. W. FOXP1: a potential therapeutic target in cancer. *Expert Opin. Ther. Targets* **11**, 955–965 (2007).
- Donmez, C. & Konac, E. Silencing effects of FOXD1 inhibit metastatic potentials of the PCA via N-cadherin – Wnt/ β -catenin crosstalk. *Gene* **836**, 146680 (2022).
- Walker, M. P. et al. FOXP1 potentiates Wnt/ β -catenin signaling in diffuse large B cell lymphoma. *Sci. Signal.* **8**, ra12 (2015).
- Mei, S., Wang, X., Zhang, J., Qian, J. & Ji, J. In vivo transfection of C/EBP- α gene could ameliorate CCL4-induced hepatic fibrosis in mice. *Hepatol. Res.* **37**, 531–539 (2007).
- Tao, L. L. et al. C/EBP- α ameliorates CCl4-induced liver fibrosis in mice through promoting apoptosis of hepatic stellate cells with little apoptotic effect on hepatocytes in vitro and in vivo. *Apoptosis* **17**, 492–502 (2012).
- Ross, S. E. et al. Inhibition of adipogenesis by Wnt signaling. *Science* **289**, 950–953 (2000). (1979).
- Wang, J. et al. TRIB2 acts downstream of Wnt/TCF in liver cancer cells to regulate YAP and C/EBP α function. *Mol. Cell* **51**, 211 (2013).
- Keeshan, K. et al. Transformation by Tribbles homolog 2 (Trib2) requires both the Trib2 kinase domain and COP1 binding. *Blood* **116**, 4948–4957 (2010).
- Grandinetti, K. B. et al. Overexpression of TRIB2 in human lung cancers contributes to tumorigenesis through downregulation of C/EBP α . *Oncogene* **30**, 3328–3335 (2011).
- PETERKOFOSKY, A. The mechanism of action of histidase: amino-enzyme formation and partial reactions. *J. Biol. Chem.* **237**, 787–795 (1962).
- Sin, Y. Y., Baron, G., Schulze, A. & Funk, C. D. Arginase-1 deficiency. *J. Mol. Med.* **93**, 1287–1296 (2015).
- Chafey, P. et al. Proteomic analysis of β -catenin activation in mouse liver by DIGE analysis identifies glucose metabolism as a new target of the Wnt pathway. *Proteomics* **9**, 3889–3900 (2009).
- Chandel, N. S. Amino acid metabolism. *Cold Spring Harb. Perspect. Biol.* **13**, a040584 (2021).
- Lee, J. S. et al. Urea cycle dysregulation generates clinically relevant genomic and biochemical signatures. *Cell* **174**, 1559–1570.e22 (2018).
- Liberti, M. V. & Locasale, J. W. The Warburg effect: how does it benefit cancer cells? *Trends Biochem. Sci.* **41**, 211–218 (2016).

42. Fischer, K. et al. Inhibitory effect of tumor cell-derived lactic acid on human T cells. *Blood* **109**, 3812–3819 (2007).
43. Wang, Z. H., Peng, W. B., Zhang, P., Yang, X. P. & Zhou, Q. Lactate in the tumour microenvironment: from immune modulation to therapy. *EBioMedicine* **73**, 103627 (2021).
44. Wang, B., Tian, T., Kalland, K. H., Ke, X. & Qu, Y. Targeting Wnt/ β -catenin signaling for cancer immunotherapy. *Trends Pharmacol. Sci.* **39**, 648–658 (2018).
45. Dobin, A. et al. STAR: ultrafast universal RNA-seq aligner. *Bioinformatics* **29**, 15–21 (2013).
46. Li, B. & Dewey, C. N. RSEM: accurate transcript quantification from RNA-Seq data with or without a reference genome. *BMC Bioinform.* **12**, 323 (2011).
47. Love, M. I., Huber, W. & Anders, S. Moderated estimation of fold change and dispersion for RNA-seq data with DESeq2. *Genome Biol.* **15**, 1–21 (2014).
48. Yamaguchi, K. et al. Bromodomain protein BRD8 regulates cell cycle progression in colorectal cancer cells through a TIP60-independent regulation of the pre-RC complex. *iScience* **26**, 106563 (2023).
49. Langmead, B. & Salzberg, S. L. Fast gapped-read alignment with Bowtie 2. *Nat. Methods* **9**, 357–359 (2012).
50. Zhang, Y. et al. Model-based analysis of ChIP-Seq (MACS). *Genome Biol.* **9**, R137 (2008).
51. Heinz, S. et al. Simple combinations of lineage-determining transcription factors prime cis-regulatory elements required for macrophage and B cell identities. *Mol. Cell* **38**, 576–589 (2010).
52. Yamaguchi, K. et al. Overexpression of cohesion establishment factor DSCC1 through E2F in colorectal cancer. *PLoS ONE* **9**, e85750 (2014).
53. Ohashi, Y. et al. Depiction of metabolome changes in histidine-starved *Escherichia coli* by CE-TOFMS. *Mol. Biosyst.* **4**, 135–147 (2008).
54. Ooga, T. et al. Metabolomic anatomy of an animal model revealing homeostatic imbalances in dyslipidaemia. *Mol. Biosyst.* **7**, 1217–1223 (2011).
55. Sugimoto, M., Wong, D. T., Hirayama, A., Soga, T. & Tomita, M. Capillary electrophoresis mass spectrometry-based saliva metabolomics identified oral, breast and pancreatic cancer-specific profiles. *Metabolomics* **6**, 78–95 (2010).
56. Yamamoto, H. et al. Statistical hypothesis testing of factor loading in principal component analysis and its application to metabolite set enrichment analysis. *BMC Bioinform.* **15**, 51 (2014).
57. Junker, B. H., Klukas, C. & Schreiber, F. Vanted: a system for advanced data analysis and visualization in the context of biological networks. *BMC Bioinform.* **7**, 109 (2006).
58. Pang, Z. et al. Using MetaboAnalyst 5.0 for LC–HRMS spectra processing, multi-omics integration and covariate adjustment of global metabolomics data. *Nat. Protoc.* **17**, 1735–1761 (2022).

Acknowledgements

We thank Yumiko Isobe, Seira Hatakeyama, and Yuqing Huang (The University of Tokyo) for their technical assistance. The super-computing resource was provided by Human Genome Center, The Institute of Medical Science, The University of Tokyo (<http://sc.hgc.jp/shirokane.html>). This work was supported by JSPS KAKENHI grant number JP20K07563 to K.Y. and Takeda Science Foundation to K.Y.

Author contributions

Conceptualization: K.Y., S.N., Y.F. Formal Analysis, S.N., K.Y. Investigation: S.N., K.Y. Methodology: S.N., K.Y., K.T., S.T., T.I., Y.F. Visualization: S.N., K.Y. Writing—Original Draft: S.N., K.Y., Y.F. Writing—Review & Editing: S.N., K.Y., K.T., S.T., T.I., Y.F. Funding Acquisition: K.Y. Supervision: K.Y., Y.F.

Competing interests

The authors declare no competing interests.

Additional information

Supplementary information The online version contains supplementary material available at <https://doi.org/10.1038/s42003-024-06202-9>.

Correspondence and requests for materials should be addressed to Kiyoshi Yamaguchi or Yoichi Furukawa.

Peer review information *Communications Biology* thanks Serif Senturk and the other, anonymous, reviewer(s) for their contribution to the peer review of this work. Primary Handling Editors: Joao Valente. A peer review file is available.

Reprints and permissions information is available at <http://www.nature.com/reprints>

Publisher's note Springer Nature remains neutral with regard to jurisdictional claims in published maps and institutional affiliations.

Open Access This article is licensed under a Creative Commons Attribution 4.0 International License, which permits use, sharing, adaptation, distribution and reproduction in any medium or format, as long as you give appropriate credit to the original author(s) and the source, provide a link to the Creative Commons licence, and indicate if changes were made. The images or other third party material in this article are included in the article's Creative Commons licence, unless indicated otherwise in a credit line to the material. If material is not included in the article's Creative Commons licence and your intended use is not permitted by statutory regulation or exceeds the permitted use, you will need to obtain permission directly from the copyright holder. To view a copy of this licence, visit <http://creativecommons.org/licenses/by/4.0/>.

© The Author(s) 2024